Remote Sensing of Environment 248 (2020) 111943

Contents lists available at ScienceDirect

Remote Sensing of Environment

journal homepage: www.elsevier.com/locate/rse

Using NASA Earth observations and Google Earth Engine to map winter cover crop conservation performance in the Chesapeake Bay watershed

Alison Thieme[a,b], Sunita Yadav[a,c], Perry C. Oddo[a,d], John M. Fitz[a,b], Sean McCartney[a,e], LeeAnn King[f], Jason Keppler[g], Gregory W. McCarty[f], W. Dean Hively[h,*]

[a] NASA DEVELOP National Program, MS 307, Hampton, VA 23681, United States
[b] University of Maryland, Department of Geographical Sciences, 2181 Samuel J. LeFrak Hall, 7251 Preinkert Drive, College Park, MD 20742, United States
[c] U.S. Department of Agriculture, Foreign Agricultural Service, 1400 Independence Avenue S.W., Washington, D.C. 20250, United States
[d] Universities Space Research Association (USRA), 7178 Columbia Gateway Drive, Columbia, MD 21046, United States
[e] Science Systems & Applications, Inc., 10210 Greenbelt Road, Suite 600, Lanham, MD 20706, United States
[f] U.S. Department of Agriculture, Agricultural Research Service, Hydrology and Remote Sensing Laboratory, Rm 104 Bldg 007 BARC-W, 10300 Baltimore Ave, Beltsville, MD 20705, United States
[g] Maryland Department of Agriculture, 50 Harry S. Truman Parkway, Annapolis, MD 21401, United States
[h] U.S. Geological Survey, Lower Mississippi-Gulf Water Science Center, Rm 104 Bldg 007 BARC-W, 10300 Baltimore Ave, Beltsville, MD 20705, United States

ARTICLE INFO

Keywords:
Google Earth Engine
Remote sensing
Cover crop
Conservation
Chesapeake Bay
Biomass
Ground cover
Adaptive management
BMP
Vegetation index

ABSTRACT

Winter cover crops such as barley, rye, and wheat help to improve soil structure by increasing porosity, aggregate stability, and organic matter, while reducing the loss of agricultural nutrients and sediments into waterways. The environmental performance of cover crops is affected by choice of species, planting date, planting method, nutrient inputs, temperature, and precipitation. The Maryland Department of Agriculture (MDA) oversees an agricultural cost-share program that provides farmers with funding to cover costs associated with planting winter cover crops, and the U.S. Geological Survey (USGS) and the U.S. Department of Agriculture-Agricultural Research Service (USDA-ARS) have partnered with the MDA to develop satellite remote sensing techniques for measuring cover crop performance. The MDA has developed the capacity to digitize field boundaries for all fields enrolled in their cover crop programs (> 26,000 fields per year) to support a remote sensing performance analysis at a statewide scal,e and has requested assistance with the associated imagery processing from the National Aeronautics and Space Administration (NASA). Using the Google Earth Engine (GEE) cloud computing platform, scripts were developed to process Landsat 5/7/8 and Harmonized Sentinel-2 imagery to measure winter cover crop performance. We calibrated cover crop performance models using linear regression between satellite vegetation indices and USGS / USDA-ARS field sampling data collected on Maryland farms between 2006 and 2012 (1298 samples). Satellite-derived Normalized Difference Vegetation Index (NDVI) values showed significant correlation with the natural logarithm of cover crop biomass ($p \leq 0.01$, $R^2 = 0.56$) and with observed percent vegetative ground cover ($p \leq 0.01$, $R^2 = 0.68$). The GEE scripts were used to composite seasonal maximum NDVI values for each enrolled cover crop field and calculate performance metrics for the winter and spring seasons of three enrollment years (2014–15, 2015–16, and 2017–18) for four Maryland counties. Results from winter 2017–18 demonstrate that rye and barley fields had higher biomass than wheat fields, and that early planting, along with planting methods that increase seed-soil contact, increased performance. The processing capabilities of GEE will support the MDA in scaling up remote sensing performance analysis statewide, providing information to evaluate the environmental outcomes associated with various agronomic management strategies. The tool can be modified for different seasonal cutoffs, utilize new sensors to capture phenology in winter and spring, and scale to larger regions for use in adaptive management of winter cover crops planted for environmental benefit.

Project support: This project was supported by the USGS Land Change Science Program within the Land Resources Mission Area, the USDA Choptank River Conservation Effects Assessment Project (CEAP), the USDA Lower Chesapeake Bay Long Term Agricultural Research (LTAR) Project; the Maryland Department of Agriculture; and the NASA DEVELOP National Program.

* Corresponding author.
E-mail address: whively@usgs.gov (W.D. Hively).

https://doi.org/10.1016/j.rse.2020.111943
Received 5 November 2018; Received in revised form 27 April 2020; Accepted 5 June 2020

1. Introduction

1.1. Background Information

The Chesapeake Bay is a diverse ecosystem supporting a wide variety of flora and fauna (Preston and Shackelford, 2002; DeLuca et al., 2004). It is the largest estuary in the United States, with tidal waters covering an area of 11,000 km^2 and a watershed of roughly 167,000 km^2 extending over six states and the District of Columbia (Fig. 1; Boesch et al., 2001). Migratory birds use the Bay as a stopover point on the Atlantic Flyway, and the fisheries are some of the most productive in the country (Mabey et al., 2005; Chesapeake Executive Council, 1990). In addition, the Chesapeake Bay watershed is home to large metropolitan areas with high population densities (Jantz et al., 2004). The associated infrastructures, urban development, and the surrounding agriculture have a large impact on the Chesapeake Bay ecosystem, often leading to reduced habitat quality and eutrophication of water bodies due to point and non-point source pollution from nutrients, sediment, and contaminants (Kemp et al., 2005; Talberth et al., 2015). "Agriculture contributes more than half of the nitrogen (primarily from animal manures, chemical fertilizers and crop fixation) transported from the watershed to the Bay" (Brakebill et al., 2014) and is linked to eutrophication and declines in macrofauna and blue crabs (Kemp et al., 2005).

The Maryland Agricultural Water Quality Cost-Share (MACS) Program, managed by the Maryland Department of Agriculture (MDA), provides cost-share grants to farmers to help offset the costs associated with the implementation of certain best management practices that address water quality concerns on Maryland farms. The Maryland Cover Crop Program (Maryland Department of Agriculture, 2019), established in 1997 as a component of MACS, incentivizes farmers to grow winter cover crops to reduce nutrient and sediment loss from farmland (Chesapeake Bay Program, 2014; Meisinger et al., 1991). In addition to these environmental benefits, planting cover crops during winter months can increase soil health, reduce pesticide usage, and increase yields for cash crops by reducing opportunistic weeds and insect pathogens (Sharma et al., 2018). The MACS program offers a variety of incentive payment rates depending on the cover crop species and agronomic management techniques used (Maryland Department of Agriculture (MDA), 2019). Cover crop performance can vary depending on planting date, seeding method, previous summer crop, field preparation, local and annual climate variability, and a variety of additional factors (Hively et al., 2009; Hively et al., 2020; Lee et al., 2016). Performance is evaluated using metrics such as aboveground biomass, percent vegetative ground cover, and nutrient uptake (Hively et al., 2009; Prabhakara et al., 2015). Higher biomass is associated with a greater amount of ground cover, which reduces soil erosion by wind and water and assists in building soil organic matter (Prabhakara et al., 2015; Snapp et al., 2005). In addition, biomass is strongly associated with nutrient uptake, with nitrogen concentrations in aboveground biomass of winter cover crops typically ranging from 2% to 4% (Hively et al., 2009). Therefore, accurate measurement of biomass in concert with chlorophyll and nitrogen content is important to understand the impacts of winter cover crops on nutrient loss from agricultural systems (Prabhakara et al., 2015). Prior research has demonstrated that early planting dates result in higher biomass accumulation, which can significantly reduce soil nitrate concentrations. Soil nitrate content can be reduced by > 80% when cover crop growth exceeds 1000 kg/ha of aboveground biomass (Hively et al., 2009; Hively et al., 2020).

The U.S. Department of Agriculture-Agricultural Research Service (USDA–ARS) and the U.S. Geological Survey (USGS) have collaborated with the MDA since 2006, developing remote sensing techniques to

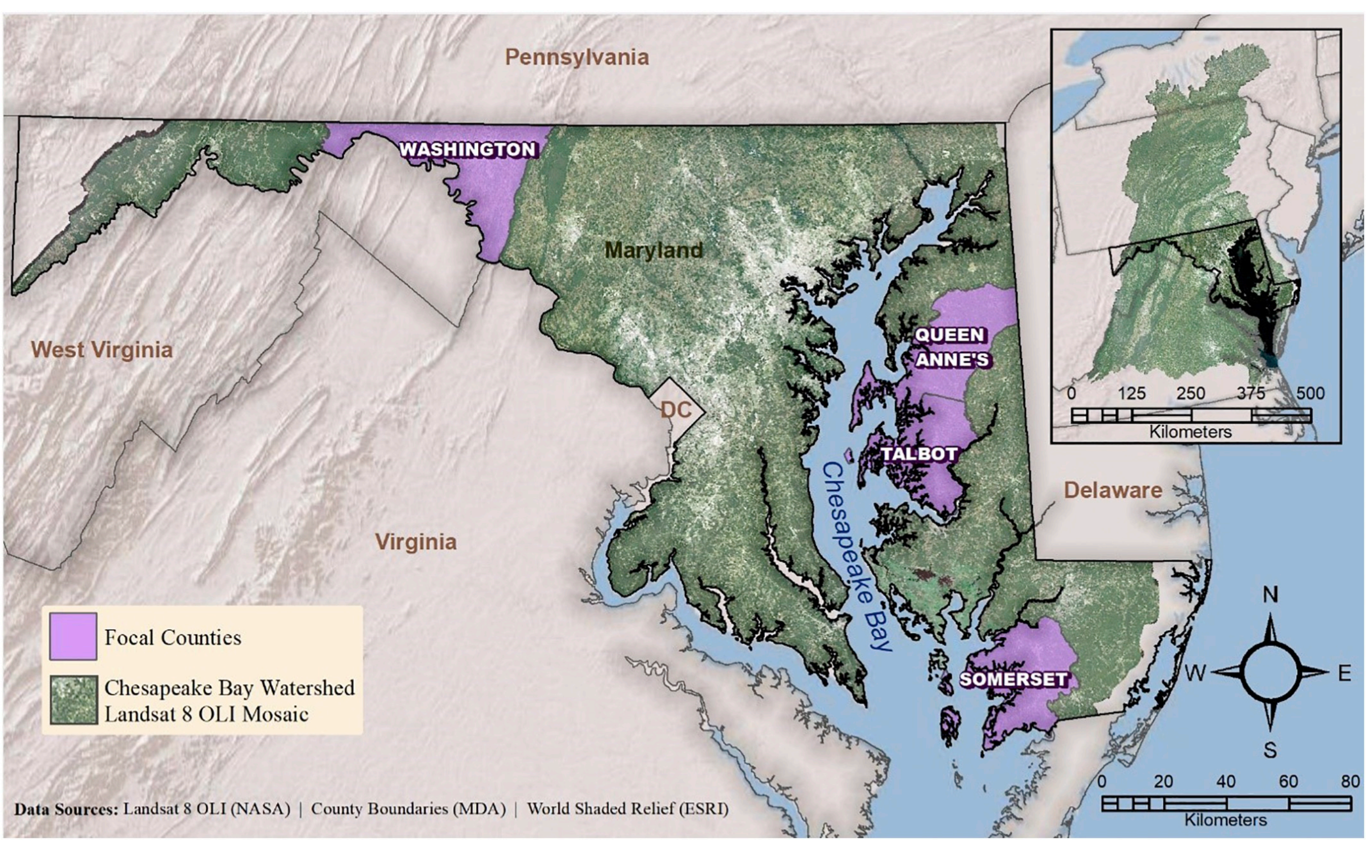

Fig. 1. Landsat 8 Operational Land Imager (OLI) mosaic of the Chesapeake Bay watershed (inset) with focal counties (Queen Anne's, Somerset, Talbot, and Washington, Maryland, USA) highlighted in purple (mosaic adapted from Taylor and Estrada, 2015). (For interpretation of the references to colour in this figure legend, the reader is referred to the web version of this article.)

assess winter cover crop performance in Maryland (Hively et al., 2009; Hunt et al., 2011; Hively et al., 2015; Prabhakara et al., 2015). The scale of the studies includes use of proximal ground sensors (Prabhakara et al., 2015), high-resolution aerial images (Hunt et al., 2011), and medium-resolution multispectral satellite data (*i.e.*, SPOT [Satellite Pour l'Observation de la Terre] 4 and 5, and Landsat 5, 7, 8; Hively et al., 2009; Hively et al., 2015). The amount of green vegetation on cover cropped fields is measured using reflectance indices such as the Normalized Difference Vegetation Index (NDVI), with calibration of satellite imagery analysis provided by on-farm sampling of cover crop performance. The MDA has developed the capacity to digitize field boundaries for MACS cover crop cost-share program enrollment, and those datasets, including related agronomic management information for each field, are shared with the USDA-ARS / USGS research team to support satellite performance analysis.

As the amount of enrolled cover crop acreage in the MACS has increased each year due to high interest from farmers, so has the MDA's interest in scalable technologies. Previous work has been successful in mapping cover crop performance in several focus areas, including Talbot County, Maryland, and in subwatersheds of the Choptank River, on the Eastern Shore of the Bay (Hively et al., 2009; Hunt et al., 2011; Prabhakara et al., 2015). However, such methods have not yet been broadly applied across the state, because the scene-specific workflow has been time consuming and difficult to scale. Furthermore, while use of commercial imagery could provide a high-resolution evaluation of cover crop performance, the frequency and cost of the amount of imagery needed would be prohibitive to scale the analysis to the entire state using traditional data processing. These barriers are beginning to be broken by research teams mapping cover crop emergence in the Midwest (Environmental Working Group, 2018; Seifert et al., 2018), but remote sensing has not yet been applied at large scale to a geospatial database containing detailed knowledge of field-specific winter cover crop agronomic management practices.

Freely available imagery such as Landsat and Sentinel-2 Earth observations from the National Aeronautics and Space Administration (NASA) and the European Space Agency (ESA) can provide an opportunity to scale the cover crop performance measurements to the entire State of Maryland. The processing demands of such an endeavor are made possible by the cloud-computing platform Google Earth Engine (GEE), which hosts both NASA and ESA surface reflectance satellite imagery (Gorelick et al., 2017).

1.2. Objectives

We seek to demonstrate the ability of an operational cloud-based system to scale MDA cover crop performance evaluation to the statewide level, using geospatial enrollment data records that were recorded by MDA in four Maryland counties (Talbot, Washington, Somerset, and Queen Anne's). We develop GEE-based analyses to obtain and process clear imagery for multiple years in the winter and spring seasons, describing the relationship between satellite-derived NDVI and on-farm field sampling data, and calculate performance metrics (aboveground biomass, vegetative ground cover) for each cover crop field, with the overall goal of characterizing the effectiveness of various agronomic management practices and informing adaptive management of conservation implementation. This collaborative effort was realized through partnerships with the USGS, the USDA–ARS, the MDA Office of Resource Conservation, the U.S. Environmental Protection Agency (EPA) Chesapeake Bay Program, and the NASA DEVELOP National Program.

2. Methodology

2.1. Data acquisition

2.1.1. Calibration data

Project partners at USGS and USDA–ARS provided *in situ* measurements of cover crop biomass and percent ground cover from data collected during on-farm field sampling in the winter (December–January) and spring (March–April) of each year from 2006 through 2012. This dataset included 711 biomass samples (423 winter, 288 spring), and 587 groundcover samples (386 winter, 201 spring). The samples were each associated with a global positioning system (GPS) point identifying the sampling location within cropland fields located on the Eastern Shore within Talbot and Queen Anne's Counties. All fields were enrolled in the MACS cover crop cost-share program (Maryland Department of Agriculture (MDA), 2018). Three sampling locations per field were established in each field, at least 40 m apart, and away from field edges and irregular features. At each sampling location, the aboveground biomass (dry weight, kg/ha) was measured by clipping vegetation from within a 0.5-m^2 quadrat and drying 24 h at 60 °C, after which samples were ground and percent nitrogen content of biomass was determined by dry combustion (LECO). Three shoulder-height (1.5 m) nadir red-green-blue (RGB) photographic images were acquired near each sampling location and were later processed using SamplePoint software (classified using 144 randomly placed crosshair locations per photo) to determine percent vegetative cover. These *in situ* data were used to develop calibration equations to translate satellite indices to estimated vegetative biomass and percent ground cover using Landsat 5 and Landsat 7 imagery acquired within two weeks of each sampling date, as described below in section 4.1. Calibration equations and model applications were applied using an R script that is freely available at https://github.com/NASA-DEVELOP/COVER. The USGS and USDA–ARS additionally provided technical knowledge of cropping systems in the study region.

2.1.2. Enrollment data

Our end users at MDA provided shapefiles identifying the boundaries of agricultural fields enrolled in the winter cover crop cost-share program, along with tabular data describing the agronomic management of each field. The agronomic data associated with each field boundary polygon included cover crop species, planting date (with early, standard, and late planting date categories defined as prior to October 1, between October 1 and October 15, and between October 15 and November 6, respectively), planting method (drilled; broadcast light disk; broadcast; aerial seeding), previous summer crop species (corn, soybean, vegetables), and field area (Table 1; Supplementary Data). Each of those agronomic management categories factors into a variable cost-share payment rate schedule established by the MDA (Maryland Department of Agriculture (MDA), 2018) and may potentially be expected to produce variable performance of the resulting cover crops. For example, planting methods that provide greater seed-soil contact (drilling, disking) are expected to result in better environmental performance (increased biomass and fractional groundcover, as measured by NDVI) than aerial seeding and broadcasting (Chesapeake Bay Program, 2016). The shapefiles included all enrolled cover cropped fields within four counties (Queen Anne's, Somerset, Talbot, Washington) for the winters of 2014–15 (5228 fields), 2015–16 (7192 fields), and 2017–18 (5580 fields). For the winter of 2016–17, the program used by MDA for geospatial data capture was in revision, and no shapefiles were available for that year. At the time of analysis, enrollment data were only available for these four counties.

Table 1
Example of Maryland Agricultural Cost-Share Program winter cover crop agronomic enrollment data.

Field ID	Species	Planting Method	Planting Date	Previous Crop
1	Wheat	Conventional tillage	27-09-2017	Corn
2	Barley	No-Till	01-10-2017	Soybeans
3	Rye	Broadcast Light Disk	15-10-2017	Sorghum
4	Canola	Broadcast Stalk-Chop	30-09-2017	Corn
5	Forage Radish	Aerial	01-11-2017	Soybeans

2.1.3. Imagery

Satellite imagery for this analysis was acquired from several sensors between the years 2006 and 2018 and was processed for analysis in GEE. Specific data included were Landsat 5 Thematic Mapper (TM; U.S. Geological Survey Earth Resources Observation and Science Center, 2012), Landsat 7 Enhanced Thematic Mapper (ETM+; U.S. Geological Survey Earth Resources Observation and Science Center, 2014a), Landsat 8 Operational Land Imager (OLI; U.S. Geological Survey Earth Resources Observation and Science Center, 2014b), and Harmonized Sentinel-2 MultiSpectral Instrument (MSI) surface reflectance images (Claverie et al., 2018). Coverage was obtained for Landsat 5 TM and Landsat 7 ETM+ for 2006–2013, Landsat 8 OLI for 2013–2018, and Sentinel-2 MSI for 2015–2018.

Imagery from NASA's Landsat Archive was obtained through GEE's interactive Code Editor. All Landsat 5 TM and Landsat 7 ETM+ images had been atmospherically corrected using the Landsat 4–7 Surface Reflectance Product generated from Landsat Ecosystem Disturbance Adaptive Processing System (LEDAPS) and Landsat 8 OLI images had been atmospherically corrected using the Landsat Surface Reflectance Code (USGS, 2018a; USGS, 2018b; Vermote et al., 2016). Landsat images were masked using a CFMask algorithm to remove identified clouds, cloud shadows, snow, and ice (Foga et al., 2017). Both the surface reflectance and CFMask algorithms are encoded into the Landsat 5, Landsat 7, and Landsat 8 Surface Reflectance (Tier 1 Level 2A) products available in GEE. This facilitated the rapid data acquisition and preprocessing of the large datasets that this project required.

Harmonized Sentinel-2 images acquired during the 2015–16 and 2017–18 cover crop seasons were downloaded from NASA (2019) and uploaded into GEE (Sentinel-2 was launched in June 2015, so imagery from that platform was not available for the 2014–15 cover crop season). The Harmonized Sentinel-2 imagery data product is created by resampling to 30 m and adjusting to match Landsat 8 spectral response and pixel resolution (Claverie et al., 2018; Skakun et al., 2018; NASA, 2019). The Harmonized Sentinel-2 images were atmospherically corrected using the Nadir Bidirectional Reflectance Distribution Function (BRDF)-Adjusted Reflectance code and masked using a "mask of cloud, cloud-shadow, snow and water mask [which is] a union of LaSRC mask and the mask generated from the Fmask algorithm" (Skakun et al., 2018).

The GEE scripts were written to access Landsat 5 TM, Landsat 7 ETM+, Landsat 8 OLI, and Harmonized Sentinel-2 data and calculate the seasonal maximum NDVI for each cover crop field boundary, as described below. At the time of this project, Sentinel-2 surface reflectance data were not available in GEE and the Harmonized Sentinel-2 product therefore had to be uploaded to support the analysis; however, the scripts were developed with the capacity to incorporate the Sentinel-2 MSI Level 2A product directly when it becomes available in GEE.

Each set of imagery was composited for winter (December 15–January 31) and for spring (March 1–April 15). For the cover crop planting year prior to availability of Sentinel-2 data (2014–15) these dates were expanded to December 15–February 15 and March 1–April 30 to compensate for the limited amount of cloud-free imagery available. Each winter and spring season contained between 55 and 82 Landsat 8 images acquired over the study area. The 2015–16 and 2017–18 seasons also included between 75 and 110 Harmonized Sentinel-2 images.

Because the field sampling data were collected from 2006-2012, but the enrollment shapefiles were digitized for 2015–2018, we used NDVI calibration data derived from 2006-2012 Landsat 5 TM and Landsat 7 ETM+ to create calibration models, described below, that were subsequently applied to 2015–2018 Landsat 8 OLI and Harmonized Sentinel-2 imagery to predict cover crop performance. The Landsat 5 TM and Landsat 7 ETM+ sensors produce similar measurements for NDVI (Vogelmann et al., 2001). However, the Landsat 8 OLI sensor exhibits small differences in reflectance values relative to Landsat 5 TM and Landsat 7 ETM+, due to differences in band width and spectral response (Chastain et al., 2019; Li et al., 2013; Roy et al., 2016). In particular, the near-infrared (NIR) band of the OLI was designed to be considerably narrower than that of ETM+ to avoid a spectral water absorption feature, resulting in slightly higher NIR reflectance and slightly higher NDVI values (Chastain et al., 2019). Roy et al. (2016) compared Landsat 7 ETM+ with Landsat 8 OLI reflectance values for 6317 overlapping image pairs collected one day apart and determined that surface reflectance NDVI values were on average 0.0164 higher for OLI than for ETM+, owing largely to differences in spectral response in the NIR. This difference, while significant, is of considerably smaller magnitude than the expected image-to-image differences arising from the relative impact of the atmosphere on Landsat ETM+ NDVI (Roy et al., 2014; Roy et al., 2016). Applying the 0.0164 average difference in OLI surface reflectance NDVI to derived wintertime cover crop performance calibration equations at NDVI = 0.50 would be expected to result in an overestimation of approximately 2% vegetated ground

Fig. 2. Workflow of methodology including data acquisition, imagery processing, enrollment data processing, model calibration, and analysis.

cover (36% *versus* 34%) and 33 kg/ha of aboveground biomass (361 *versus* 328 kg/ha). For greatest accuracy, future applications might consider collecting on-farm calibration data contemporaneous with Landsat 8 data acquisition or applying transformation equations developed in Roy et al. (2016) to convert OLI NDVI values into ETM+ equivalent values.

Similarly, the Sentinel-2 Multi Spectral Instrument (MSI) produces slightly higher NDVI readings than the Landsat 8 OLI, due to differences in bandwidth and spectral response (Zhang et al., 2018). To correct for this, NASA supplies Harmonized Sentinel-2 imagery that has been adjusted to match OLI spatial and spectral characteristics (Claverie et al., 2018) and produce similar values for NDVI. To test the compatibility of the calibration with Harmonized Sentinel-2 data, we compared 1882 NDVI values from enrolled fields obtained from Harmonized Sentinel-2 and Landsat 8 OLI images acquired on the same day; this comparison yielded an R^2 value of 0.98 with a slope of 0.994 and intercept of 0.001, indicating excellent alignment between the data sets.

2.2. Data processing

We used the image collections uploaded into GEE to apply the CFmask algorithm to surface reflectance imagery (Foga et al., 2017). After masking out clouds, cloud shadows, water and snow, NDVI was calculated for each image:

$$\mathrm{NDVI} = (\mathrm{NIR} - \mathrm{Red})/(\mathrm{NIR} + \mathrm{Red}) \tag{1}$$

The NDVI (Rouse et al., 1974; Tucker, 1979) is a commonly used index that correlates well with the leaf area index of green vegetation (Gowda et al., 2015; Kang et al., 2016). Although additional vegetation indices could be derived from the satellite imagery, Prabhakara et al. (2015) compared nine indices for measurement of winter cover crop biomass and percent vegetative ground cover on Maryland field sites and determined that NDVI was the top performing index. Therefore, our analysis relied on NDVI for performance calculations.

Field boundaries within each year's MDA cover crop enrollment database were buffered inward by 15 m from the edge of each field to reduce mixed pixel edge effects (Fig. 2). The outcome of the 15-m buffer was to remove from analysis any pixels that intersected the true field boundary. The resulting buffered field boundaries were overlaid onto each Landsat 8 OLI, Landsat 7 TM, and Landsat 5 TM and Harmonized Sentinel-2 image falling within the corresponding winter and spring season, and the average NDVI value within each field was recorded, along with the imagery date. The field-specific average NDVI values were collected from every available cloud masked image within the seasonal ranges and saved in a tabular data file. From these spatially averaged NDVI values, temporal maximums within each year and season were gathered, and the image date associated with each field's maximum NDVI was recorded. The calculation of average NDVI within each field smoothed out any in-field variation in performance, and while in-field variation is relevant at the scale of precision agricultural management, the averaging was deemed a reasonable solution for calculation of performance metrics at a landscape scale. The maximum NDVI values were subsequently used for cover crop performance analysis, described below. The team encoded the data acquisition, processing, and analysis in a GEE script that is freely available at https://github.com/NASA-DEVELOP/CCROP.

Any enrolled field boundaries without valid satellite data coverage were deleted from the analysis. The occurrence of missing data due to extensive cloudiness (pixels with cloud cover in all images incorporated into a seasonal composite) was minimal, with less than 0.05% of cropland pixels missing valid NDVI data for the season-years with both Landsat and harmonized Sentinel (2015–16 and 2017–18), rising to 1.7% (winter) and 0.4% (spring) of cropland pixels missing valid NDVI data for the year with only Landsat data available (2014–15). However, when cloudiness was combined with snow cover, and fields with NDVI < 0.0 were removed from analysis, this resulted in removal of 0.6% to 7.6% of enrolled fields for years without Sentinel imagery availability, while all fields had valid data for years with harmonized Sentinel and Landsat availability (Supplementary Data). The mapped performance of any individual field does not affect MDA payment rates or otherwise directly impact the farmer, and therefore the loss of information for fields that were removed or only partially covered by valid imagery was not judged to be a major concern.

In comparison to the GEE scripts, traditional methods of data processing would include downloading individual Landsat images, calculating NDVI, overlaying the vector file of enrollment data, extracting average values for each field for 15–20 images, determining the maximum NDVI value for each field within the time sequence, and applying calibration equations to calculate biomass and vegetative ground cover, each of which would be an independent processing step. By using GEE, the time required to accomplish this workflow was greatly shortened, from several days of work using traditional methods to several hours using the GEE workflow, despite the fact that GEE is rather slow at handling polygon shapefiles.

For the *in situ* field dataset, sampling point locations identified with sub-meter GPS (Trimble GeoXT) were overlaid on Landsat surface reflectance imagery for the temporally nearest single cloud-free image to the field sampling date, and the associated NDVI values and imagery dates were extracted into a tabular calibration database that included field-sampled biomass and ground cover data (Supplementary Data).

2.3. Calibration development

For the *in situ* field sampling dataset, calibration regression equations were developed between the measured performance variables (*i.e.* cover crop biomass and percent vegetative ground cover) and satellite-derived NDVI. To account for the non-linear relationship between biomass and leaf area index and observed saturation above NDVI = 0.80 (Prabhakara et al., 2015), a natural logarithmic transformation was applied to the biomass measurements, resulting in the following biomass calibration model:

$$\ln(\mathrm{biomass}) = \mathrm{NDVI} + \varepsilon \tag{2}$$

where ε represents model error.

Note that when converting from predicted ln(biomass) to biomass, a delogging adjustment factor should be applied to account for bias during exponentiation (Miller, 1984):

$$\mathrm{biomass} = e^{(\ln(\mathrm{biomass}) + \mathrm{MSE}/2)} \tag{3}$$

where MSE is mean square error from analysis of variance (ANOVA) results.

For vegetative ground cover, the relationship with NDVI is linear, with both the fractional ground cover measurements and the vegetation index saturating above 80% ground cover (Prabhakara et al., 2015), and the following calibration model was used to determine fractional vegetative ground cover:

$$\%\mathrm{vegetative\ ground\ cover} = \mathrm{NDVI} + \varepsilon \tag{4}$$

where ε represents model error.

The calibration dataset included $n = 711$ biomass samples (winter samples $n = 423$, collected in December or January of 2006–2012; springtime samples $n = 288$, collected in April or May of 2006–2012) and $n = 587$ vegetative ground cover samples (winter samples $n = 386$, collected in December or January of 2006–2012; springtime samples $n = 201$, collected in April or May of 2006–2012), and seasonal regression equations were derived for each performance factor.

To test for calibration *versus* validation of results, a data splitting method, without replacement, was employed to randomly split the data into 70% for calibration and 30% for validation, and this random grouping was performed 10 separate times. The calibration:validation datasets were then used to evaluate NDVI linear regression models for ln(biomass) and for vegetative ground cover, in the winter and spring seasons.

3. Results & discussion

3.1. Biomass and percent ground cover models

Results (Table 2, Fig. 3a, c) showed a reasonably strong relationship between NDVI and ln(biomass), with adjusted R^2 of 0.562 and Root Mean Square Error (RMSE) of 0.782 (equivalent to 2.19 kg/ha) for the wintertime regression, and adjusted R^2 of 0.403 and RMSE of 0.803 (equivalent to 2.23 kg/ha) for the springtime regression. Results (Table 2, Fig. 3b, d) showed a stronger association between NDVI and percent vegetative ground cover with adjusted R^2 of 0.685 and RMSE of 13.05 for the wintertime regression, and adjusted R^2 of 0.624 and RMSE of 14.66 for the springtime regression.

Predictive accuracy was greater for percent ground cover ($R^2 = 0.624$ to 0.685) than for biomass ($R^2 = 0.403$ to 0.562) likely because ground cover has a linear, non-saturating relationship with NDVI (as vegetation covers a greater portion of the soil, NDVI increases), whereas biomass exhibits a non-linear saturating relationship with NDVI (biomass is affected by the ratio of leaf to stem, thickness of leaves, and leaf angle distribution, and a greater 'depth' of vegetation covering the soil can greatly increase biomass without greatly affecting reflectance from the field surface).

Several factors influenced the goodness of fit for the calibration equations. The data were collected on a broad variety of farm fields, with different soil types and under varying soil moisture conditions, on different dates spanning six years. Additionally, the relationship between NDVI and cover crop biomass can be impacted by chlorosis, dormancy, and frost damage that happens under cold weather conditions (Prabhakara et al., 2015). Within any individual sampling-imagery date pair, goodness of fit improved somewhat, ranging from 0.54 to 0.77 with best results obtained for 90 samples in the winter of 2008–2009. When comparing date-specific regressions, slopes associated with ln(biomass) varied from 4.34 to 7.86 (average 5.57) and intercepts varied from 0.99 to 4.46 (average 3.27). When the various sampling dates are combined, the overall goodness of fit declines, likely due to the impact of soil moisture variability among dates, along with any atmospheric effects that are not accounted for in the conversion to surface reflectance (Low et al., 2015; Tian et al., 2015; Yang and Lo, 2000). Ideally, remote sensing analysis of cover crop performance would be calibrated by field data collection that occurred within each particular season of analysis. However, such data were not collected in 2014–2018, and so analysis of cover crop performance relied upon seasonal calibration equations derived from the 2006–2012 multi-year field sampling dataset.

Model residuals did not display any structure for estimation of ln (biomass) or for percent vegetative ground cover, indicating that the assumptions required for linear regression were met and the regressions were appropriate for the data (Supplemental Materials Fig. A). The model fits were weaker at the lower data range for predicting biomass, and weaker at the lower and upper data ranges for predicting percent vegetative ground cover but were strong in the central range.

Some of the observed variance could be explained by including a second variable (deltaGDD4) that measured the number of growing degrees (base temperature of 4 °C) accumulated between the day of field sample collection and the satellite acquisition date used to calculate NDVI:

$$\ln(\text{biomass}) = \text{NDVI} + \text{deltaGDD4} + \varepsilon \quad (5)$$

and

$$\text{vegetative ground cover} = \text{NDVI} + \text{deltaGDD4} + \varepsilon \quad (6)$$

where ε represents model error. Weather data used to calculate GDD4 were obtained from a weather station located at the University of Maryland Wye Research Station (38°54″31′ N; 76°08″38′ W; University of Maryland, 2018).

Including the deltaGDD4 variable improved model adj. R^2 by only 0.03 and 0.08 for winter and spring ln(biomass) models, and by 0.01 for the winter ground cover models, and the term was not statistically significant for the spring ground cover model, leading to the conclusion that temporal differences between sampling and imagery acquisition were not of great consequence. Additionally, the deltaGDD4 variable was not applicable to the seasonal cover crop enrollment prediction models, for which only satellite NDVI values were available. Therefore, the final seasonal calibration equations relied solely upon NDVI (Eqs. (2) and (4)).

The statistical output for the ten 70:30 calibration:validation model runs are provided in Supplemental Materials Table A. All of the calibration and validation models were highly significant (p-value $< 2 \times 10^{-16}$) with somewhat greater variance in spring compared to winter (biomass model adj. R^2 range: 0.54–0.59 for winter and 0.35–0.46 for spring; percent vegetative cover model Adj. R^2 range: 0.64–0.69 for winter and 0.62–0.73 for spring). Likewise, RMSE values generally displayed lower values for winter models in comparison to spring models. Overall, the variation among each of the 10 calibration:validation iterations was small (Supplementary Materials Table A), and the equations resulting from the average of the 10 validation runs were very similar to the calibration equations derived from the complete dataset. For instance, for an NDVI of 0.40, the 10-run average equation estimates a percent groundcover of 24.581%, while the complete dataset equation estimates a percent groundcover of 24.618%, which is a negligible difference well within the margins of rounding to relevant significant digits. Because the average 70:30 calibration:validation results were negligibly different from the regression equations derived using the entire dataset, the equations listed in Table 2, derived using all data points, were used for prediction of cover crop performance.

3.2. Predicting cover crop performance on enrolled fields

The maximum seasonal NDVI associated with each cover crop enrolled field boundary, derived from imagery processing in GEE, was transformed using the equations detailed in Table 2 to calculate estimated cover crop biomass and percent vegetative ground cover for each field, for each of the three years of enrollment data. The resulting cover crop performance metrics were then associated with the agronomic management information for each field record. In this way, satellite-derived estimates of cover crop performance could be used to evaluate the comparative environmental effectiveness of various agronomic

Table 2
Calibration model results predicting natural log of biomass (ln(biomass)) and percent vegetative ground cover from satellite-derived Normalized Difference Vegetation Index (NDVI) values, including adjusted R^2 (adj. R^2) and degrees of freedom (df).

Performance variable	Season	Model	Adj. R^2	RMSE	df
Cover crop biomass	Winter	ln(biomass) = 3.2022 + 5.3740 * NDVI	0.562	0.782	422
	Spring	ln(biomass) = 4.7794 + 3.7453 * NDVI	0.403	0.803	288
Vegetative ground cover	Winter	% cover = −21.904 + 116.305 * NDVI	0.685	13.050	386
	Spring	% cover = −10.783 + 107.566 * NDVI	0.624	14.663	201

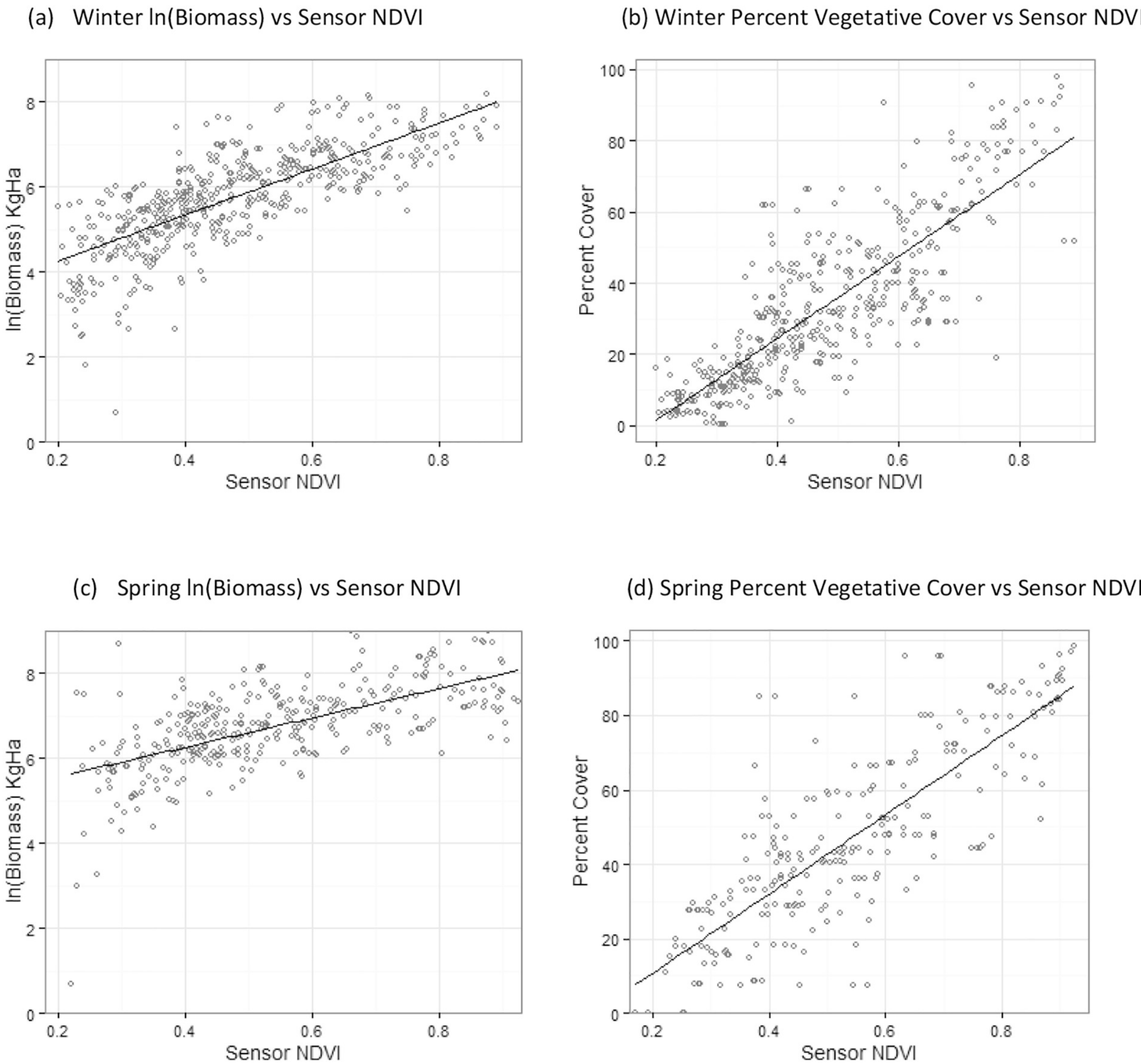

Fig. 3. Relationship between satellite-derived NDVI and cover crop performance variables (biomass, percent vegetative cover) using Landsat surface reflectance to calculate sensor NDVI, and a dataset of 1298 cover crop field samples to measure performance: a) wintertime ln(biomass) *versus* NDVI; b) wintertime percent vegetative ground cover *versus* NDVI; c) springtime ln(biomass) *versus* NDVI; and d) springtime percent vegetative ground cover *versus* NDVI.

cover crop management strategies at the landscape scale. An example map of cover crop performance is provided in Figs. 4 and 5, showing results for a collaborating farm that has released its cover crop enrollment records for public use.

It should be noted that the increased temporal frequency of satellite imagery acquisition provided by integration of Landsat 8 and Harmonized Sentinel-2 imagery proved critical to robust characterization of cover crop performance. When seasonal maximum NDVI

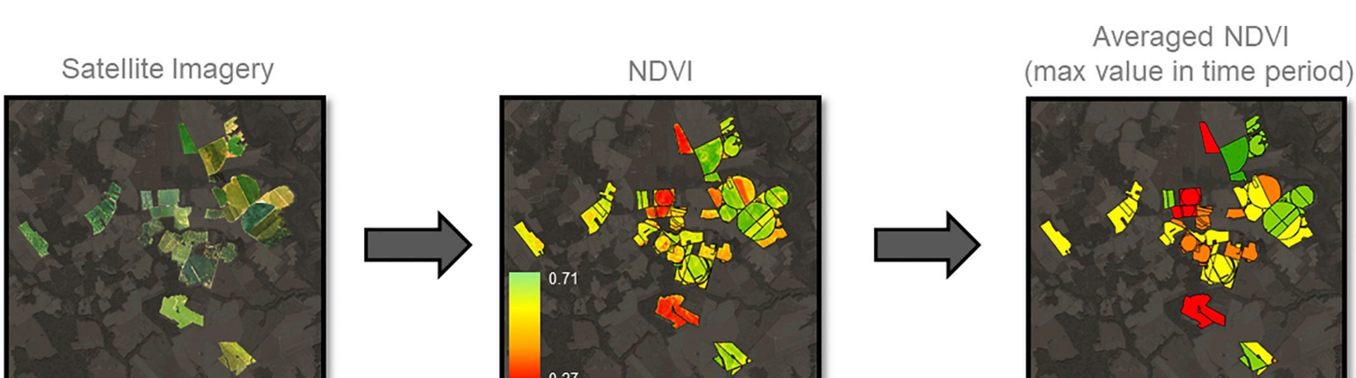

Fig. 4. Example of conversion of satellite imagery to maximum averaged NDVI (collaborating farm, Talbot County, MD).

composites were calculated separately for Landsat 8 and for Harmonized Sentinel 2 (Fig. 6), the two imagery sources combined to provide greater coverage of valid data (eliminating fields with NDVI < 0.2 in one of the two imagery sources) and a cluster of points became apparent in the springtime where high cirrus clouds had decreased Sentinel NDVI values below 0.2 without triggering the cloud mask (Fig. 6b). By combining the two satellite data sources, the composite maximum NDVI values provided a more accurate picture of cover crop performance.

3.3. Summarizing seasonal cover crop performance

After the satellite reflectance indices were used to calculate winter and springtime cover crop performance measures for each field enrolled in the MACS Program, these field-specific results were segmented by county, season, and year, and then summarized for each category of agronomic management (Table 3 and Supplemental Materials Tables B through M). Spatial autocorrelations in cover crop performance occur in the natural landscape, due to localized differences in soils, cropping systems, and climate. Additionally, inter-annual variability in winter cover crop performance can be large, owing to differences in annual weather conditions. For example, Hively et al., 2020 found that the warmth of the winter season had a greater impact on wintertime greenness on the Eastern Shore of Maryland than did the acreage of cover crop implementation. However, within a county, within a particular season, within a particular year, the effects of spatial and temporal autocorrelation are expected to be limited. The use of counties as the spatial unit of analysis helps to compensate for spatial autocorrelation, and the segmentation of analysis into winter and spring seasons of each individual year assists to compensate for temporal autocorrelation.

An example of the performance output is given for Queen Anne's County, Maryland, for the 2017-18 cover crop period, in Table 3. Output tables for the remaining counties and years are included in Supplemental Materials Tables B through M. Significant differences among factor levels were computed for mean NDVI values using analysis of variance (ANOVA) followed by Tukey's Least Significant Difference, as indicated by letter codes in Table 3 where factor levels with the same letter (within factor type) are not significantly different and factor levels with different letters were found to be significantly different with > 95% confidence. Detailed statistical results supporting the development of the letter codes are provided in Supplemental Materials Table N.

Measured environmental performance of cover crops (biomass, percent vegetative ground cover) varied based on planting date, species, planting method, and previous crop (Table 3; Supplemental Materials Tables B through M). In general, crops planted early (prior to October 1) and during the standard planting period (October 1-October 15) outperformed crops planted later in the fall (Table 3; Supplemental Materials Tables B through M), likely due to greater availability of warm weather suitable for growth (Hively et al., 2020). In the winter of 2017, late-planted cover crops provided only 45% of the biomass and

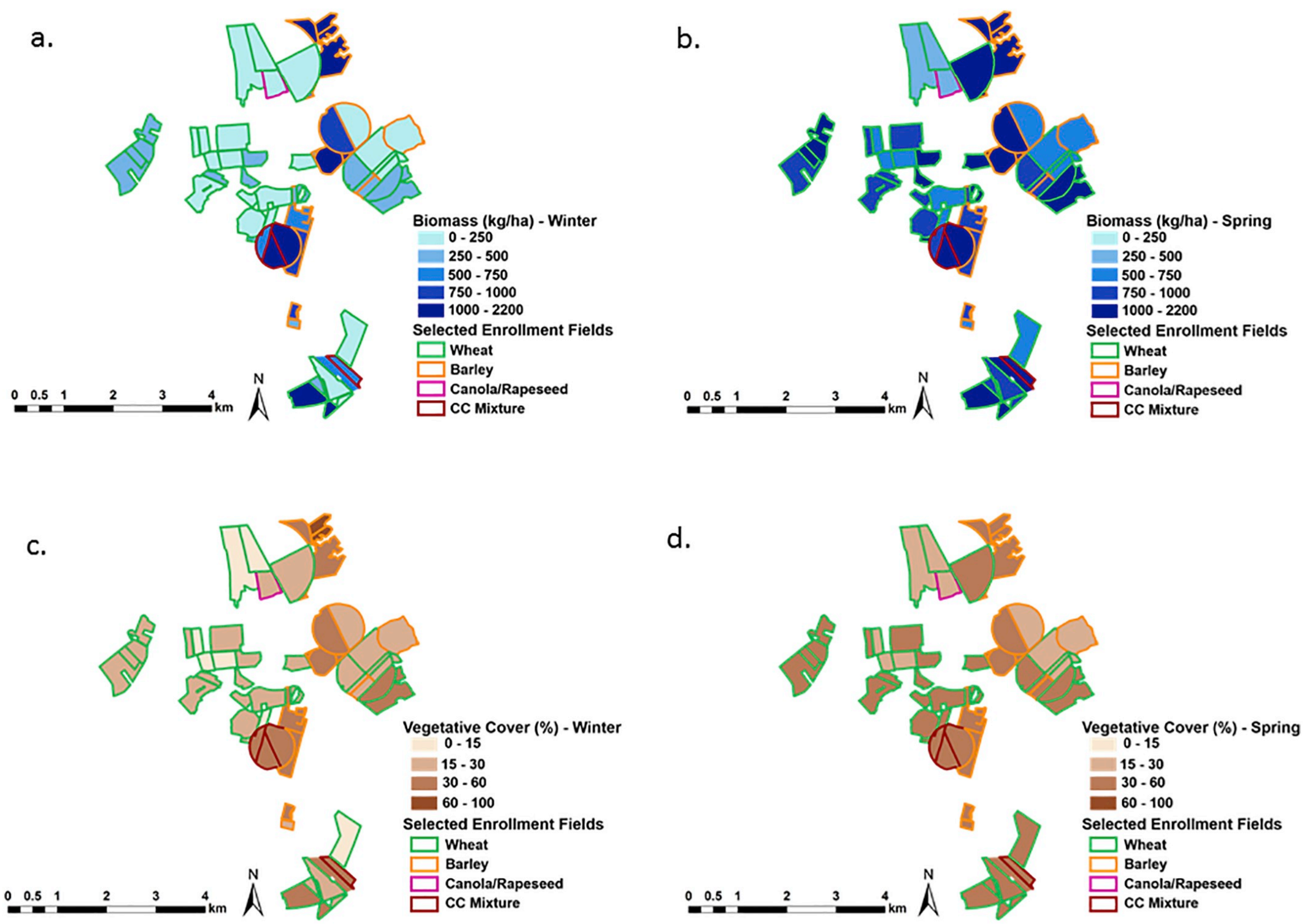

Fig. 5. Predicted cover crop performance on example cover cropped fields for a) winter biomass, b) spring biomass, c) winter ground cover, and d) spring ground cover, for the winter (December 15, 2017–January 31, 2018) and spring (March 1, 2018–April 15, 2018) seasons. These site-specific cover crop cost-share enrollment data have been released for public use by the collaborating farm.

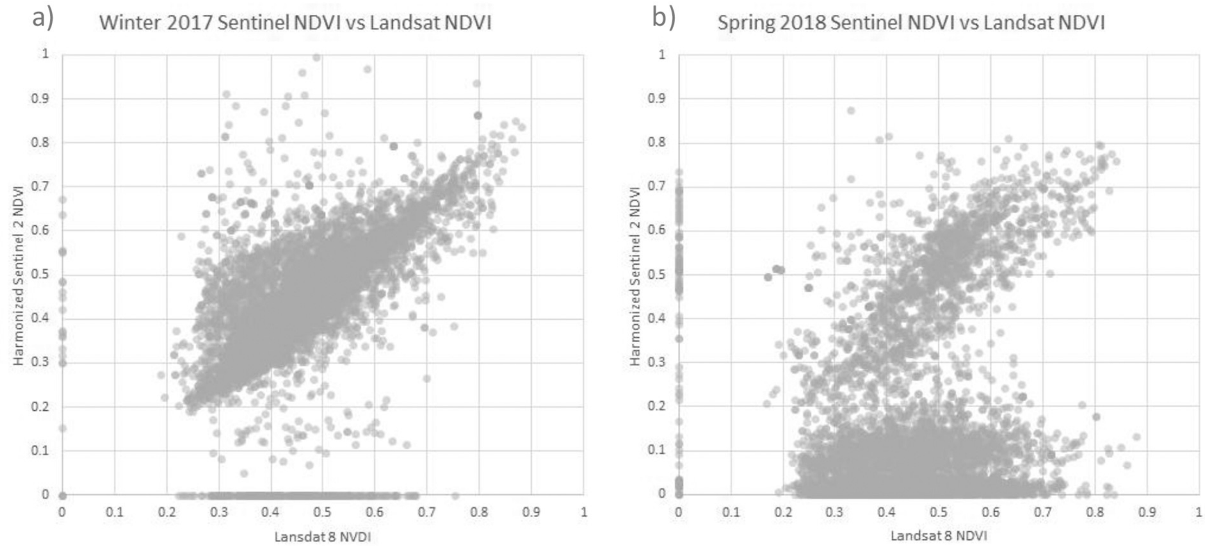

Fig. 6. NDVI values for enrolled cover crop fields derived from Landsat 8 *versus* Harmonized Sentinel-2 maximum NDVI composite imagery for a) winter (December 15, 2017–January 31, 2018), and b) spring (March 1, 2018–April 15, 2018).

Table 3
Agronomic performance of winter cover crops in Queen Anne's County, Maryland for 2017–18 during a) winter and b) spring seasons.

Agronomic Factor	Enrolled Fields #	Enrolled Fields ha	Average NDVI	*	Predicted Biomass (kg/ha)	Predicted Ground Cover (%)
a) Wintertime (December 15, 2017 to January 31, 2018)						
Species						
Wheat	1336	32,448	0.48	a	607	34
Rye	318	7853	0.52	b	820	38
Barley	58	1363	0.52	b	912	38
Planting Date						
Early (By September 30)	812	20,490	0.53	a	852	39
Standard (By October 15)	663	15,477	0.49	b	642	36
Late (After October 15)	529	12,811	0.42	c	384	27
Planting Method						
Aerial	800	20,390	0.47	bc	519	33
Broadcast Light Tillage	239	4570	0.49	bc	750	35
Broadcast Stalk Chop	20	294	0.52	abc	736	39
Conventional Drill	86	1637	0.59	a	1381	46
No-till Drill	453	11,084	0.52	b	815	39
Previous Crop						
Corn	1235	32,437	0.51	a	758	37
Soybean	687	14,186	0.45	b	462	31
Vegetable	41	1107	0.58	c	1262	46
All Fields	2004	48,778	0.49		659	35
b) Springtime (March 1, 2018 to April 15, 2018).						
Species						
Wheat	1336	32,448	0.45	a	993	37
Rye	318	7853	0.48	bc	1192	41
Barley	58	1363	0.45	ac	963	37
Planting Date						
Early (By September 30)	812	20,490	0.44	a	1004	37
Standard (By October 15)	663	15,477	0.47	b	1130	40
Late (After October 15)	529	12,811	0.41	c	859	34
Planting Method						
Aerial	800	20,390	0.42	c	861	34
Broadcast Light Tillage	239	4570	0.48	b	1185	41
Broadcast Stalk Chop	20	294	0.45	bc	955	38
Conventional Drill	86	1637	0.56	a	1707	50
No-till Drill	453	11,084	0.46	b	1068	39
Previous Crop						
Corn	1235	32,437	0.45	a	1041	38
Soybean	687	14,186	0.43	b	943	36
Vegetable	41	1107	0.49	a	1145	42
All Fields	2004	48,778	0.45		1007	37

*Within each factor, groupings with different letters have significantly different mean NDVI values at $p < .05$ while groupings with identical letters are not different.

69% of the groundcover provided by early-planted cover crops (Table 3a). Early-planted cover crops outperformed standard planting dates in the wintertime, indicating increased performance in the critical early winter leaching period, but standard-planted cover crops surpassed early-planted cover crops in the spring analysis (Table 3b), likely due to increased susceptibility of the more mature early-planted crops to wintertime frost damage. Although effect of planting date varied by year and county, largely similar results were found for other years and counties (Supplemental Materials Tables B through M). The effect of planting method was also apparent, with the method that provided the best soil preparation and seed-soil contact ("conventional drill") outperforming other planting methods, and with aerial and broadcast seeding exhibiting reduced performance (Table 3). The conventional drill planting method outperformed all others in 14 out of 16 county-season-year combinations (Supplemental Materials Tables B through M). In Queen Anne's County, for the 2017-18 cover crop period, rye and barley outperformed wheat in the winter analysis, likely due to their greater cold tolerance (Table 3a). However, wheat made up the majority (78%) of cover crop plantings despite its comparatively poor winter performance. The species-related differences were less pronounced in the springtime analysis, although rye outperformed the other species (Table 3b). Finally, cover crops planted in fields that had produced vegetables or corn in the previous season consistently outperformed than those grown on soybean fields (Table 3; Supplemental Materials Tables B through M), likely due to increased availability of residual soil nitrate (Chesapeake Bay Program, 2016).

In the winter of 2017 wheat was the most frequently planted crop in Queen Anne's County, but performance metrics indicate it was outperformed by fields planted with rye and barley (Table 3). By further examining the performance of cover crop species by planting date category, we see that late planted wheat was the second most common practice (26% of all fields) but performed most poorly in terms of predicted biomass and percent ground cover (Table 4). There is evidently an opportunity to increase the effectiveness of the winter crop program by shifting away from late-planted wheat toward early planting dates and more cold-tolerant species such as rye and barley.

Tabular output for each county, season, and year of remote sensing analysis was transferred to stakeholders at the MDA, for their use in analyzing patterns of agronomic performance. This information can inform potential adjustments to cost-share incentive rates to promote the most environmentally impactful cover crop management practices. The methodology established here can provide a basis for rapid, operational performance calculations in each coming year, for all fields enrolled in the MACS winter cover crop cost-share program throughout Maryland (> 25,000 fields per year covering > 300,000 ha of farmland).

3.4. Limitations

While this analysis dramatically improves upon the current capabilities of the MDA to assess cover crop performance, it has some notable limitations that could be improved through further investigation. The field calibration dataset used to derive the regression models associating satellite reflectance indices with cover crop performance variables was limited in spatial extent to counties on the Eastern Shore of Maryland and may not accurately represent landscape conditions in the western counties. Furthermore, there is a temporal separation between the date range of calibration data collection (2006–2013) and the application of predictive models (2014–2019), creating a potential risk of systematic error due to changes in agricultural management techniques. Therefore, collection of additional field data is needed to develop more precise calibration models for statewide analysis.

It should be noted that while it is quite effective at imagery processing, GEE can be slow in its handling of polygons. The analysis of statewide cover crop performance, including creation of composite seasonal NDVI imagery and overlay with > 25,000 polygon field boundaries, takes approximately 2 h, which is substantially less time than would be required to complete the analysis through graphics user

Table 4

Agronomic performance of winter cover crops by species and planting date in Queen Anne's County, Maryland for a) winter and b) spring time periods of the 2017-18 cover crop season.

Species and Planting Date	Enrolled Fields		NDVI	*	Predicted Biomass	Predicted Ground Cover
	#	ha			(kg/ha)	(%)
a) Wintertime (December 15, 2017 to January 31, 2018).						
Wheat						
Early (Before Oct 1)	397	10,031	0.53	b	796	40
Standard (Oct 1–15)	502	11,489	0.50	d	663	36
Late (Oct 15 - Nov 6)	425	10,598	0.42	c	374	27
Rye						
Early (Before Oct 1)	124	3237	0.59	a	1236	47
Standard (Oct 1–15)	116	2883	0.48	cd	622	34
Late (Oct 15 - Nov 6)	79	1734	0.46	c	457	31
Barley						
Early (Before Oct 1)	35	1035	0.57	ab	1255	45
Standard (Oct 1–15)	23	328	0.44	cd	390	29
Late (Oct 15 - Nov 6)	0	0	–		–	–
b) Springtime (March 1, 2018 to April 15, 2018).						
Wheat						
Early (By September 30)	397	10,031	0.45	a	994	38
Standard (By October 15)	502	11,489	0.48	ef	1153	41
Late (After October 15)	425	10,598	0.41	b	816	33
Rye						
Early (By September 30)	124	3237	0.52	c	1371	45
Standard (By October 15)	116	2883	0.45	af	1037	37
Late (After October 15)	79	1734	0.47	ace		40
Barley						
Early (By September 30)	35	1035	0.46	acde	1066	39
Standard (By October 15)	23	328	0.42	*cf*	807	34
Late (Oct 15 - Nov 6)	0	0	–	a	–	–

*Within each factor, groupings with different letters have significantly different mean NDVI values at $p < .05$ while groupings with identical letters are not significantly different.

interface-based processing. Once the overall seasonal analysis is complete, producing maps and summary statistics on a county-by-county basis takes approximately 5 min per county to display results; therefore, the user needs to be patient when operating the report creation interface. Perhaps a more optimum computational framework would be to use GEE to produce the seasonal composite imagery and initial seasonal performance analysis for enrolled cover crop field boundaries, and then to create county and watershed-specific performance tables and graphical analysis using a statistical program such as R.

Within this study, NDVI was a useful metric for aboveground biomass and percent vegetative ground cover. It would also be useful to directly measure the chlorophyll and nitrogen content of winter cover crops, which are more strongly correlated with indices that incorporate the red edge reflectance bands (Lamb et al., 2002) that are available from satellites such as Sentinel-2 MSI, an instrument that had not yet launched when the current calibration dataset was collected. Future investigations could benefit from collecting in-field measurements of cover crop nitrogen and chlorophyll content, in addition to biomass and percent ground cover, to calibrate a remotely sensed measurement of winter cover crop nitrogen content.

4. Conclusions

The MDA's Cover Crop Program is a critical component of the statewide initiative to improve the health of the Chesapeake Bay. As the number and acreage of enrolled fields continues to rise, it is increasingly important to ensure that fields are compliant with program requirements and to understand which management practices are most effective. The use of cloud-based satellite processing techniques allowed for the extraction of performance metrics associated with each cover crop field in the MDA cost-share enrollment database for specific seasonal time periods. The increased frequency of imagery acquisiton provided by harmonized integration of Sentinel and Landsat was critical to providing good temporal coverage within the seasonal target periods. The satellite-derived estimates of biomass and percent vegetative ground cover were used to characterize the effect of various agronomic management practices on cover crop performance. The resulting insights can inform how the choice of cover crop species, planting date, planting method, and previous crop impact the environmental performance of a given field. By monitoring cover crop performance in counties across Maryland, and working with stakeholders to improve conservation implementation, the MDA is supporting the overarching goal of reducing nutrient and sediment runoff in the Chesapeake Bay watershed.

Automating the methodology using Google Earth Engine has allowed partners at the MDA to dramatically reduce the time required to complete the necessary imagery processing steps, requiring hours instead of days to compile each season's cover crop performance data. Wide scale adoption of this methodology beyond the four counties discussed in this analysis could dramatically improve the efficiency with which compliance is verified and performance is tracked. As such, the scripts created for this project have been released to the project partners, end-users, and to the public on GitHub following the NASA DEVELOP software release protocol. The data processing workflow and GEE scripts enable the MDA to evaluate the performance of enrolled cover crops on an annual basis, and to assess and improve long-term environmental impacts of winter cover crops throughout Maryland.

4.1. Future directions

Currently, the MDA visits 30% of all enrolled fields in the fall to verify cover crop implementation, and 20% of enrolled farms in the spring to verify cover crop termination compliance (Keppler, 2017). Using remote sensing imagery to evaluate implementation for all fields enrolled in the program would allow the MDA to assess winter cover crop performance in both the winter and spring months, support adaptive management of their cover crop incentive program, and potentially replace required field visits with imagery-based verification of management dates and practices.

Two subsequent NASA DEVELOP projects have streamlined and automated the workflow developed here to create a simple and effective GEE user interface for use by the MDA (and other stakeholders). This user interface compiles cover crop performance results and identifies fields with unusually low cover crop performance to target field visits to identify the cause. Reasons for low cover crop performance can include the factors characterized by the agronomic dataset (*e.g.*, planting date, planting method, species, previous crop, and previous crop manure application and irrigation status) as well as extraneous factors including grazing by geese, low soil nitrogen, and unfavorable weather. The combined output of the NASA DEVELOP projects will complete the development and release of a package of GEE-based software to fully support the MDA in incorporating near real-time satellite remote sensing into the winter cover crop cost-share program. The resulting information documenting cover crop performance, communicated in a useful format, can aid in the understanding and improvement of agronomic methods used to manage cover crops. The MDA plans to use the generated information to support adaptive management of their cover crop incentive program and to identify underperforming fields. By identifying underperforming fields and measuring cover crop termination dates, the MDA will be able to check for program adherence, identify reasons for the poor performance, adapt cost share structures, and communicate the results to participating farmers to improve winter cover crop environmental performance.

Sentinel-2 MultiSpectral Instrument Level-2A surface reflectance products are currently being ingested by GEE. Once these data are available, they can be incorporated into an operational cover crop remote sensing process in place of the Harmonized Sentinel-2 product used in this manuscript.

Declaration of Competing Interest

The authors declare that they have no known competing financial interests or personal relationships that could have appeared to influence the work reported in this paper.

Acknowledgments

This project addressed NASA's Agriculture application area within the Applied Sciences Program by implementing timely, calibrated satellite data analysis to assess winter cover crop effectiveness. The work completed here is a collaboration between NASA DEVELOP, USGS, USDA–ARS, and the MDA.

We thank Alisha Mulkey and Dawn Bradley from the Maryland Department of Agriculture for providing cover crop enrollment data and guidance on data interpretation. We would also like to thank the collaborating farm for allowing their fields to be displayed in our visualizations, and are grateful to the many Eastern Shore farmers and soil conservation district offices for allowing access to cover crop fields for biomass sampling. Finally, we thank our DEVELOP science advisor, Dr. John Bolten at NASA Goddard Space Flight Center.

Any opinions, findings, and conclusions or recommendations expressed in this material are those of the authors and do not necessarily reflect the views of the National Aeronautics and Space Administration.

This material is based upon work supported by NASA through contract NNL16AA05C and cooperative agreement NNX14AB60A. Additional support for this project was provided by the USGS Land Change Science Program within the Land Resources Mission Area, the USDA Choptank River Conservation Effects Assessment Project, the USDA Lower Chesapeake Long Term Agricultural Research project, and by the Maryland Department of Agriculture. Any use of trade, firm, or

product names is for descriptive purposes only and does not imply endorsement by the U.S. Government.

Appendix A. Supplementary data

Supplementary data to this article can be found online at https://doi.org/10.1016/j.rse.2020.111943. The supporting dataset has been published at http://dx.doi.org/10.17632/cbgkpyxvjz.1.

References

Boesch, D.F., Brinsfield, R.B., Magnien, R.E., 2001. Chesapeake Bay eutrophication. J. Environ. Qual. 30 (2), 303–320.

Brakebill, P.J., Ator, S., Blomquist, J., 2014. Science Summary—Sources, Fate, and Transport of Nitrogen and Phosphorus in the Chesapeake Bay Watershed—Interpretations and Applications of Spatially Referenced Regression on Watershed Attributes (SPARROW) Nutrient Model Results. pp. 13.

Chastain, R., Housman, I., Goldstein, J., Finco, M., Tenneson, K., 2019. Empirical cross sensor comparison of sentinel-2A and 2B MSI, Landsat-8 OLI, and Landsat-7 ETM+ top of atmosphere spectral characteristics over the conterminous United States. Remote Sens. Environ. 221 (2019), 274–285.

Chesapeake Bay Program, 2014. Cover Crops: One Key to Reducing Nutrients to the Bay. Chesapeake Bay Program, Annapolis, MD. http://www.chesapeakebay.net/blog/post/cover_crops_one_key_to_reducing_nutrients_to_bay.

Chesapeake Bay Program, 2016. Cover Crops Practices for use in Phase 6.0 of the Chesapeake Bay Program Watershed Model. https://www.chesapeakebay.net/documents/Phase_6_CC_EP_Final_Report_12-16-2016-NEW_TEMPLATE_FINAL.pdf.

Chesapeake Executive Council, 1990. Chesapeake Bay Waterfowl Policy and Management Plan (Rep.). US EPA, Annapolis, MD.

Claverie, M., Ju, J., Masek, J.G., Dungan, J.L., Vermote, E.F., Roger, J.-C., Skakun, S.V., Justice, C., 2018. The harmonized Landsat and Sentinel-2 surface reflectance data set. Remote Sens. Environ. 219, 145–161. https://doi.org/10.1016/j.rse.2018.09.002.

DeLuca, W.V., Studds, C.E., Rockwood, L.L., Marra, P.P., 2004. Influence of land use on the integrity of marsh bird communities of Chesapeake Bay, USA. Wetlands 24 (4), 837–847. https://doi.org/10.1672/0277-5212(2004)024[0837:IOLUOT]2.0.CO;2.

Environmental Working Group, 2018. Mapping cover crops on corn and soybeans in Illinois, Indiana, and Iowa. pp. 2015–2016. https://www.ewg.org/research/mapping-cover-crops-corn-and-soybeans-illinois-indiana-and-iowa-2015-2016.

Foga, S., Scaramuzza, P.L., Guo, S., Zhu, Z., Dilley, R.D., Beckmann, T., Schmidt, G.L., Dwyer, J.L., Hughes, M.J., Laue, B., 2017. Cloud detection algorithm comparison and validation for operational Landsat data products. Remote Sens. Environ. 194, 379–390. https://doi.org/10.1016/j.rse.2017.03.026.

Gorelick, N., Hancher, M., Dixon, M., Ilyushchenko, S., Thau, D., Moore, R., 2017. Google earth engine: planetary-scale geospatial analysis for everyone. Remote Sens. Environ. 202, 18–27. https://doi.org/10.1016/j.rse.2017.06.031.

Gowda, P., Oommen, T., Misra, D., Schwartz, R., Howell, T., Wagle, P., 2015. Retrieving leaf area index from remotely sensed data using advanced statistical approaches. GIScie. Remote Sens. 4, 156.

Hively, W.D., Lang, M., McCarty, G.W., Keppler, J., Sadeghi, A., McConnell, L.L., 2009. Using satellite remote sensing to estimate winter cover crop nutrient uptake efficiency. J. Soil Water Conserv. 64 (5), 303–313. https://doi.org/10.2489/jswc.64.5.303.

Hively, W.D., Duiker, S., McCarty, G., Prabhakara, K., 2015. Remote sensing to monitor cover crop adoption in southeastern Pennsylvania. J. Soil Water Conserv. 70 (6), 340–352.

Hively, W.D., Lee, S., Sadeghi, A., McCarty, G.W., Yeo, I.-Y., Moglen, G., 2020. Estimating the effect of winter cover crops on nitrogen leaching using cost-share enrollment data, satellite remote sensing, and Soil and Water Assessment Tool (SWAT) modeling. J. Soil Water Conserv. 75 (3), 362–375. https://doi.org/10.2489/jswc.75.3.362. (in press).

Hunt, E.R., Hively, W.D., McCarty, G.W., Daughtry, C.S.T., Forrestal, P.J., Kratochvil, R.J., Carr, J.L., Allen, N.F., Fox-Rabinovitz, J.R., Miller, C.D., 2011. NIR-green-blue high-resolution digital images for assessment of winter cover crop biomass. GISci. Remote Sens. 48, 86–98. https://doi.org/10.2747/1548-1603.48.1.86.

Jantz, C.A., Goetz, S.J., Shelley, M.K., 2004. Using the sleuth urban growth model to simulate the impacts of future policy scenarios on urban land use in the Baltimore-Washington metropolitan area. Environ. Plan. B 31 (2), 251–271. https://doi.org/10.1068/b2983.

Kang, Y., Özdoğan, M., Zipper, S., Román, M., Walker, J., Hong, S., ... Miyata, A., 2016. How universal is the relationship between remotely sensed vegetation indices and crop leaf area index? A global assessment. Remote sensing 8 (7), 597.

Kemp, W.M., Boynton, W.R., Adolf, J.E., Boesch, D.F., Boicourt, W.C., Brush, G., et al., 2005. Eutrophication of Chesapeake Bay: historical trends and ecological interactions. Mar. Ecol. Prog. Ser. 303, 1–29.

Keppler, J., 2017. Personal Communication. Retrieved 2017.

Lamb, D.W., Steyn-Ross, M., Schaare, P., Hanna, M.M., Silvester, W., Steyn-Ross, A., 2002. Estimating leaf nitrogen concentration in ryegrass (Lolium spp.) pasture using the chlorophyll red-edge: theoretical modelling and experimental observations. Int. J. Remote Sens. 23 (18), 3619–3648.

Lee, S., Yeo, I.-Y., Sadeghi, A.M., McCarty, G.W., Hively, W.D., Lang, M.W., 2016. Impacts of watershed characteristics and crop rotations on winter cover crop nitrate-nitrogen uptake capacity within agricultural watersheds in the Chesapeake Bay region. PLoS One 11 (6), e0157637. https://doi.org/10.1371/journal.pone.0157637.

Li, P., Jiang, L., Feng, Z., 2013. Cross-comparison of vegetation indices derived from Landsat-7 enhanced thematic mapper plus (ETM+) and Landsat-8 operational land imager (OLI) sensors. Remote Sens. 6, 310–329.

Low, F., Knofel, P., Conrad, C., 2015. Analysis of uncertainty in multi-temporal object-based classification. ISPRS J. Photogram. Remote Sens. 105 (July 2015), 91–106. https://doi.org/10.1016/j.isprsjprs.2015.03.004.

Mabey, S., Watts, B., Paxton, B., Smith, F., Truitt, B., Dawson, D., 2005. Characterizing stopover sites of migrating passerine birds in the lower Chesapeake Bay region for conservation: an integrated radar-habitat study. In: One Hundred and Twenty-Third Stated Meeting of the American Ornithologists' Union: abstract book (pp. 138) (abstr-), Retrieved from. http://pubs.er.usgs.gov/publication/5211311.

Maryland Department of Agriculture (MDA), 2018. Maryland's 2018–19 Cover Crop Sign Up. Maryland Department of Agriculture, Annapolis, MD. https://mda.maryland.gov/resource_conservation/counties/2018CCSignup.pdf.

Maryland Department of Agriculture (MDA), 2019. Maryland's Cover Crop Program. Maryland Department of Agriculture. https://mda.maryland.gov/resource_conservation/pages/cover_crop.aspx.

Meisinger, J.J., Hargrove, W.L., Mikkelsen, R.L., Williams, J.R., Benson, V.W., 1991. Effects of cover crops on groundwater quality.. p. 57–68. In: Hargrove, W.L. (Ed.), Cover Crops for Clean Water. Proc. Int. Conf., Jackson, TN. 9–11 Apr. 1991. Soil and Water Conserv. Soc, Ankeny, IA.

Miller, Don M., 1984. Reducing transformation bias in curve fitting. The American Statistician, May 1984 38 (2), 124–126.

National Aeronautics and Space Administration (NASA), 2019. Harmonized Landsat Sentinel-2. https://hls.gsfc.nasa.gov/.

Prabhakara, K., Hively, W.D., McCarty, G.W., 2015. Evaluating the relationship between biomass, percent groundcover and remote sensing indices across six winter cover crop fields in Maryland, United States. Int. J. Appl. Earth Obs. Geoinf. 39, 88–102. https://doi.org/10.1016/j.jag.2015.03.002.

Preston, B.L., Shackelford, J., 2002. Multiple stressor effects on benthic biodiversity of Chesapeake Bay: implications for ecological risk assessment. Ecotoxicology 11, 85–99.

Rouse, J.W., Haas, R.W., Schell, J.A., Deering, D.W., Harlan, J.C., 1974. Monitoring the Vernal Advancement and Retrogradation (Greenwave Effect) of Natural Vegetation. NASA/GSFC Type-III Final Report, Greenbelt, Maryland, U.S.A., pp. 164.

Roy, D.P., Wulder, M., Loveland, T., Woodcock, C., Allen, R., Anderson, M., ... Zhu, Z., 2014. Landsat-8: Science and product vision for terrestrial global change research. Remote Sensing of Environment 145, 154–172. https://doi.org/10.1016/j.rse.2014.02.001.

Roy, D.P., Kovalskyy, V., Zhang, H.K., Vermote, E.F., Yan, L., Kumar, S.S., Egorov, A., 2016. Characterization of Landsat-7 to Landsat-8 reflective wavelength and normalized difference vegetation index continuity. Remote Sens. Environ. 185 (2016), 57–70.

Seifert, C.A., Azzari, G., Lobell, D.B., 2018. Satellite detection of cover crops and their effects on crop yield in the Midwestern United States. Environ. Res. Lett. 13, 064033. https://doi.org/10.1088/1748-9326/aaf933.

Sharma, P., Singh, A., Singh Kahlon, C., Singh Brar, A., Grover, K.K., Dia, M., Steiner, R.L., 2018. The role of cover crops towards sustainable soil health and agriculture—a review paper. Am. J. Plant Sci. 9 (9). https://doi.org/10.4236/ajps.2018.99140. 2018.

Skakun, S.V., Ju, J., Claverie, M., Roger, J.-C., Vermote, E.F., Franch, B., Dungan, J.L., Masek, J.G., 2018. Harmonized Landsat-8 Sentinel-2 (HLS) Product User's Guide. National Aeronautics and Space Administration (NASA), Washington, DC, USA, pp. 1.4.

Snapp, S.S., Swinton, S.M., Labarta, R., Mutch, D., Black, J.R., Leep, R., Nyiraneza, J., O'Neil, K., 2005. Evaluating cover crops for benefits, costs and performance within cropping system niches. Agron. J. 97 (1), 322–332.

Talberth, J., Selman, M., Walker, S., Gray, E., 2015. Pay for performance: optimizing public investments in agricultural best management practices in the Chesapeake Bay watershed. Ecol. Econ. 118, 252–261.

Taylor, M., Estrada, L.M., 2015. Chesapeake Bay watershed. In: NASA's Scientific Visualization Studio, Retrieved from. http://svs.gsfc.nasa.gov/4366.

Tian, F., Fensholt, R., Verbesselt, J., Grogan, K., Horion, S., Wang, Y., 2015. Evaluating temporal consistency of long-term global NDVI datasets for trend analysis. Remote Sens. Environ. 163 (15 June 2015), 326–340.

Tucker, C., 1979. Red and photographic infrared linear combinations for monitoring vegetation. Remote Sens. Environ. 8, 127–150.

U.S. Geological Survey, 2018a. Landsat 4–7 Surface Reflectance (LEDAPS) Product. [Data set]. U.S. Geological Survey. https://www.usgs.gov/media/files/landsat-4-7-surface-reflectance-code-ledaps-product-guide.

U.S. Geological Survey, 2018b. Landsat 8 Surface Reflectance Code (LaSRC) Product. [Data set]. U.S. Geological Survey. https://www.usgs.gov/media/files/landsat-8-surface-reflectance-code-lasrc-product-guide.

U.S. Geological Survey Earth Resources Observation and Science Center, 2012. Landsat 4–5 TM Level-2 Surface Reflectance (SR) Science Product [Data Set]. U.S. Geological Survey. https://doi.org/10.5066/F7KD1VZ9.

U.S. Geological Survey Earth Resources Observation and Science Center, 2014a. Landsat 7 ETM+ Level-2 Surface Reflectance (SR) Science Product [Data Set]. U.S. Geological Survey. https://doi.org/10.5066/F7Q52MNK.

U.S. Geological Survey Earth Resources Observation and Science Center, 2014b. Landsat 8 OLI Level-2 Surface Reflectance (SR) Science Product [Data Set]. U.S. Geological Survey. https://doi.org/10.5066/F78S4MZJ.

University of Maryland, 2018. Weather Data for the Wye REC. University of Maryland, College of Agriculture and Natural Resources, College Park, MD. https://agnr.umd.edu/research/resources/weather-data/weather-data-wye-rec.

Vermote, E., Justice, C., Claverie, M., Franch, B., 2016. Preliminary analysis of the performance of the Landsat 8/OLI land surface reflectance product. Remote Sens. Environ. 185 (2016), 46–56. https://doi.org/10.1016/j.rse.2016.04.009.

Vogelmann, J.E., Helder, D., Morfitt, R., Choate, M.J., Merchant, J.W., Bulley, H., 2001. Effects of landsat 5 thematic mapper and landsat 7 enhanced thematic mapper plus radiometric and geometric calibrations and corrections on landscape characterization. Remote Sens. Environ. 78, 55–70. https://doi.org/10.1016/S0034-4257(01)00249-8.

Yang, X., Lo, C.P., 2000. Relative radiometric normalization performance for change detection from Multi-Date Satellite Images. Photogramm. Eng. Remote. Sens. 66 (8), 967–980 August 2000.

Zhang, H.K., Roy, D.P., Yan, L., Li, Z., Huang, H., Vermote, E., Skakun, S., Roger, J.-C., 2018. Characterization of sentinel-2A and Landsat-8 top of atmosphere, surface, and nadir BRDF adjusted reflectance and NDVI differences. Remote Sens. Environ. 215 (2018), 482–494. https://doi.org/10.1016/j.rse.2018.04.031.

Glossary

ANOVA: Analysis of Variance
BRDF: Bidirectional Reflectance Distribution Function
EPA: U.S. Environmental Protection Agency
ESA: European Space Agency
ETM: Enhanced Thematic Mapper Plus (Landsat 7)
GEE: Google Earth Engine
GDD4: Growing Degree Days
GPS: Global Positioning System
GSFC: Goddard Space Flight Center (NASA)
LEDAPS: Landsat Ecosystem Disturbance Adaptive Processing System
MACS: Maryland Agricultural Water Quality Cost-Share Program
MDA: Maryland Department of Agriculture
MSE: Mean Square Error
MSI: Multispectral Instrument (Sentinel-2)
NASA: National Aeronautics and Space Administration
NIR: Near-infrared
NDVI: Normalized Difference Vegetation Index
OLI: Operational Land Imager (Landsat 8)
RGB: Red-Green-Blue
RMSE: Root Mean Square Error
SPOT: Satellite Pour l'Observation de la Terre (“Satellite for observation of Earth”)
TM: Thematic Mapper (Landsat 5)
USDA–ARS: United States Department of Agriculture - Agricultural Research Service
USGS: U.S. Geological Survey